Novel Redox-Active Polycarbazole-Functionalized Polycatechol Network Films Produced by Controlled Electropolymerization

Yao Huang,[1] Baoyang Lu,[2] Jingkun Xu,[1] Guang Zhu,[1] Shuai Chen,[1] Ruirui Yue[1]

[1]Jiangxi Key Lab of Organic Chemistry, Jiangxi Science & Technology Normal University, Nanchang 330013, China
[2]School of Pharmacy, Jiangxi Science & Technology Normal University, Nanchang 330013, China

ABSTRACT: A novel precursor, 1,2-bis[6-(9H-carbazol-9-yl)hexyloxy] benzene (BCHB), was successfully synthesized. Its polycarbazole-functionalized polycatechol network films, poly{1,2-bis[6-(9H-carbazol-9-yl)hexyloxy] benzene} (PBCHB), with good redox activity were formed by the direct anodic oxidation of BCHB in CH_2Cl_2 and boron trifluoride diethyl etherate binary solvent solution. Ultraviolet–visible spectroscopy, Fourier transform infrared spectroscopy, ^{1}H-NMR, and matrix-assisted laser desorption ionization–time of flight mass spectrometry were used to characterize the polymers. The results indicate that the network polymers could be synthesized electrochemically with different polymerized units by controlled electropolymerization. The PBCHB films prepared at low potential were oligomers with short conjugation lengths and were soluble in common organic solvents, whereas the polymers with long conjugation lengths and hyperbranched network structures obtained at high potential were insoluble. The electrosynthesized polymers exhibited blue emission maxima around 450 nm and were much more redshifted than their monomer. The emissions were also brighter; this indicated the polymers are potential good blue-light emitters. © 2012 Wiley Periodicals, Inc. J Appl Polym Sci 000: 000–000, 2012

Key words: electrochemistry; films; fluorescence; FT-IR; MALDI

INTRODUCTION

Conjugated polymers as functional materials are now considered a very important class of electroactive and photoactive materials because of their novel electrochemical and chemical properties; these properties lead to extensive applications, such as supercapacitors, light-emitting devices, field effect transistors, sensors, resist materials, electrochromic devices, and charge storage devices.[1–11] The properties of conducting polymers strongly depend on their structural characteristics. Thus, it is necessary to develop new materials with new properties not only for fundamental investigation but also for practical applications.

O-Phenylene polymers, such as poly(*o*-dimethoxybenzene), poly(1-hydroxy-2-methoxybenzene), and polycatechol, constitute fundamental classes of conjugated structures that possess nice redox activity, good thermal stability, and fluorescence properties.[12–15] On the other hand, the substitution at the N position of polycarbazole provides an opportunity to improve both the solubility and functionality of the resulting polymers.[16–19] Because of its large conjugated structure and special photoelectronic properties, the carbazole group has been extensively used as a functional substituent in photorefractive materials, photoconductors, nonlinear optical materials, and hole-transport and light-emissive materials for organic light-emitting diodes. It was found that the length of flexible bridging chain connected with the two conjugated units has an important influence on the polymer film. Through control of the chain length and flexibility of the bridging group, one can not only avoid the formation of excimers and aggregation in conjugated polymers but also adjust the mechanical properties and the spectral response of the flexible films. With a longer bridging chain, a higher mechanical strength and longer conjugated chains in the polymer film can be obtained.[20] Therefore, it can be expected that an alkyl-bridged carbazole with a catechol monomer might result in a novel polymer with the advantages of both

Scheme 1 Synthetic route and chemical structure of BCHB (r.t. = room temperature).

polycatechol and polycarbazole. It has been known that the oxidation potential of catechol is lower than that of carbazole.[12,21] Therefore, according to variations of the oxidation potentials between catechol and carbazole units, a polycarbazole-functionalized polycatechol polymer should be obtained by the control of the electrochemical deposition conditions.

In this study, 1,2-bis[6-(9H-carbazol-9-yl)hexyloxy] benzene (BCHB; Scheme 1) was synthesized and electrochemically polymerized in CH_2Cl_2–70% boron trifluoride diethyl etherate (BFEE; by volume) at different constant applied potentials (Scheme 2). The electrochemical behavior, structural characterization, solubility, and spectroscopic properties of the as-formed poly{1,2-bis[6-(9H-carbazol-9-yl)hexyloxy] benzene} (PBCHB) films were investigated in detail.

EXPERIMENTAL

Materials

Carbazole (Shanghai Chemical Reagent Plant, technical grade, Shanghai, China) was recrystallized before use. Catechol (Tianjin Bodi Chemicals Co., Ltd., analytical grade, Tianjin, China), 1,6-dibromohexane (Acros Organics, 98%, Belgium), ammonia (Beijing Changyang Chemical Plant, 25%, Beijing, China), 18-crown-6 (Shanghai Jingchun Reagent Co., Ltd., analytical grade, Shanghai, China), tetrabutyl ammonium bromide (Tianjin Bodi Chemicals, analytical grade, Tianjin, China), and dimethyl sulfoxide (DMSO; Tianjin Bodi Chemicals, analytical grade, Tianjin, China) were used as received without further purification. Dichloromethane was purchased from Tianjin Bodi Chemicals (Tianjin, China) and was purified by distillation over calcium hydride before use. BFEE (Beijing Changyang Chemical Plant, Beijing, China) was purified by distillation before use.

Monomer synthesis

Synthesis of 9-(6-bromohexyl)-9H-carbazole[22]

1,6-Dibromohexane (4.74 mL, 30 mmol), tetrabutyl ammonium bromide (260 mg, 0.8 mmol), and aque-

ous NaOH (50%, 10 mL) were added to a 250-mL, three-necked flask containing carbazole (3.34 g, 20 mmol) in DMSO (30 mL). The mixture was stirred at room temperature for 12 h. The organic phase was separated and washed by water (60 mL) and then dried with anhydrous $MgSO_4$. The solvent was removed *in vacuo*, and the residue was purified by flash column chromatography with petroleum ether as eluent to afford white needle crystals (3.98 g, 60%; Scheme 1).

^{1}H-NMR (400 MHz, $CDCl_3$, δ): 8.10 (d, $^3J_{HH}$ = 8.2 Hz), 7.47 (t, $^3J_{HH}$ = 12.4 Hz), 7.40 (d, $^3J_{HH}$ = 8.0 Hz), 7.24 (t, $^3J_{HH}$ = 20.4 Hz), 4.32 (t, $^3J_{HH}$ = 16.6 Hz), 3.36 (t, $^3J_{HH}$ = 16.2 Hz), 1.90 (t, $^3J_{HH}$ = 16.2 Hz), 1.82 (t, $^3J_{HH}$ = 12.4 Hz), 1.46 (t, $^3J_{HH}$ = 16.2 Hz), 1.41 (t, $^3J_{HH}$ = 8.0 Hz).

Synthesis of BCHB[23]

A mixture of 9-(6-bromohexyl)-9H-carbazole (4.43 g, 14 mmol), catechol (0.48 g, 4.4 mmol), potassium carbonate (2.11 g, 15.2 mmol), and 18-crown-6 (0.43 g, 1.6 mmol) in 60 mL of anhydrous acetone was refluxed with vigorous stirring under nitrogen for 60 h. The mixture was cooled to room temperature, and the solvent was evaporated under reduced pressure. The residue was extracted between CH_2Cl_2 and deionized water. Afterward, the aqueous layer was extracted with CH_2Cl_2 (150 mL). The combined extracts were dried with anhydrous $MgSO_4$ and evaporated. The residue was purified by silica gel column chromatography (1 : 10 petroleum ether/ acetic ether) to afford the monomer (2.35 g, 89%) as a white solid (Scheme 1).

^{1}H-NMR (400 MHz, $CDCl_3$, δ): 8.01 (d, $^3J_{HH}$ = 8.0 Hz), 7.36 (t, $^3J_{HH}$ = 16.4 Hz), 7.29 (d, $^3J_{HH}$ = 8.2 Hz), 7.14 (t, $^3J_{HH}$ = 16.2 Hz), 6.78 (d, $^3J_{HH}$ = 4.4 Hz), 4.17
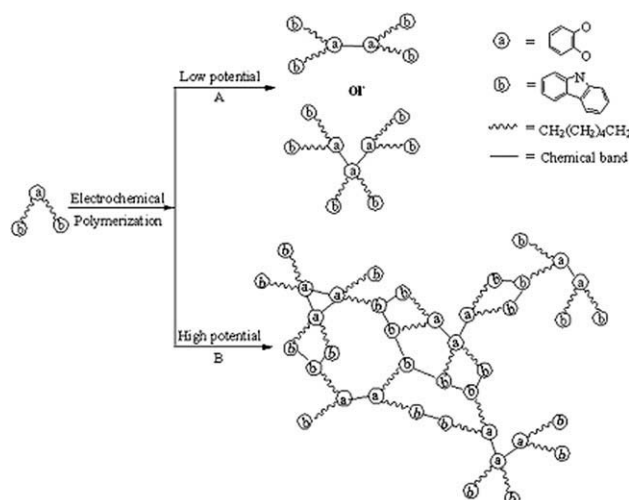
Scheme 2 Schematic view of possibilities for coupling between the carbazole unit and catechol unit.

(t, $^3J_{HH}$ = 16.0 Hz), 3.87 (t, $^3J_{HH}$ = 12.2 Hz), 1.77 (t, $^3J_{HH}$ = 16.0 Hz), 1.68 (t, $^3J_{HH}$ = 16.4 Hz), 1.42 (t, $^3J_{HH}$ = 16.0 Hz), 1.33 (t, $^3J_{HH}$ = 12.2 Hz).

Electrochemical polymerization

All of the electrochemical experiments were performed in a one-compartment cell with the use of a model 263 potentiostat–galvanostat (EG&G Princeton Applied Research, Berwyn, United States). The working and counter electrodes for the cyclic voltammetric experiments were platinum wires, both with diameters of 0.5 mm, placed 0.5 cm apart. For large-scale polymer film production, platinum and stainless steel sheets with surface areas of 1.5 and 2 cm^2 were employed as a working electrode and counter electrode, respectively. The stainless steel sheet was polished with abrasive paper (1500 mesh) and was then washed with acetone before each examination. All potentials were referred to an Ag/AgCl electrode. The potential of an Ag/AgCl reference electrode depends on the chloride ion concentration in the solution to which the electrode is exposed. The typical electrolytic solution was CH_2Cl_2–70 vol % BFEE containing 0.05M monomer, in which BFEE was used as the supporting electrolyte, and no other salts were added. The polymer films were deposited on indium tin oxide (ITO)-coated glasses for spectral measurements in the solid state.

Characterization

Ultraviolet-visible (UV–vis) spectra were taken with a PerkinElmer Lambda 900 UV–vis–near infrared spectrophotometer (Waltham, MA, United States). Fourier transform infrared (FTIR) spectra were recorded with a Bruker Vertex 70 FTIR spectrometer with KBr pellets (Bruker Optik GmbH, Ettlingen, Germany). The ^{1}H-NMR spectra were recorded on a Bruker AV 400NMR spectrometer, and $CDCl_3$ was used as the solvent (Bruker Optik GmbH, Ettlingen, Germany). The fluorescence properties were determined with a Hitachi F-4500 fluorescence spectrophotometer (Tokyo, Japan). Matrix-assisted laser desorption ionization (MALDI)–time of flight (TOF) mass spectrometry (MS) was carried out on a Bruker MICROFLEX mass spectrometer (Bruker Optik GmbH, Ettlingen, Germany). Thermogravimetric analysis (TGA) was performed with a Pyris Diamond thermogravimetry (TG)/dynamic thermal analyzer (PerkinElmer, Waltham, MA, United States). Scanning electron microscopy (SEM) measurements were taken with a JEOL JSM-6700F scanning electron microscope (Tokyo, Japan).

RESULTS AND DISCUSSION

Electrochemical synthesis of the PBCHB films

Figure 1 shows the anodic polarization curves of the BCHB monomer in CH_2Cl_2 with 10, 30, 50, 70, and
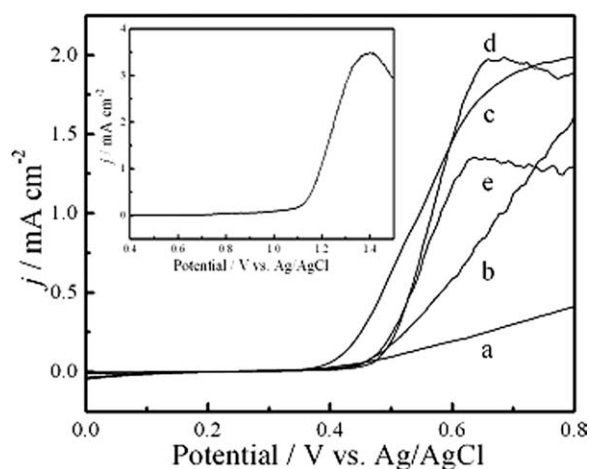

Figure 1 Anodic polarization curves of BCHB in mixed electrolytes of CH_2Cl_2 with (a) 10, (b) 30, (c) 50, (d) 70, and (e) 90 vol % BFEE, and CH_2Cl_2–0.1 mol/L Bu_4NBF_4 (insert) containing 0.05M monomer (potential scan rate = 50 mV/s). j is the current density, and $j_{p.a}$ and $j_{p.c}$ denote the anodic and cathodic peak current densities, respectively.

90 vol % BFEE and containing 0.1 mol/L Bu_4NBF_4 (insert). In the binary solvent solutions, the onset oxidation potentials of BCHB were all much lower than that in CH_2Cl_2–0.1 mol/L Bu_4NBF_4, as shown in Figure 1. The potential decrease in CH_2Cl_2 solution with BFEE could be attributed to the catalytic effect of the Lewis acid on the deprotonation of BCHB.[24] Generally, a lower oxidation potential onset can lead to easier oxidation of the monomers at given applied potential. This indicated that the oxidations of BCHB in CH_2Cl_2–BFEE were much easier than that in CH_2Cl_2. Because of this, CH_2Cl_2–BFEE was a better medium for the electropolymerization of BCHB.

The successive cyclic voltammograms (CVs) of 0.05 mol/L BCHB on a Pt wire electrode in the mixed electrolytes are shown in Figure 2. According to the previous literature,[12,21] the initial oxidation potential of catechol is much lower than that of carbazole. Therefore, peak A was assigned to the oxidation of the catechol unit, and peak B was the oxidation of the carbazole unit of the precursor. As shown in Figure 2(a,b), the CVs of BCHB in CH_2Cl_2 with 10 and 30 vol % BFEE only exhibited a single pair of redox waves. However, polymer films were still formed on the working electrode. Significantly different from those shown in Figure 2(a,b), the CVs of BCHB in CH_2Cl_2 with 50, 70, and 90 vol % BFEE exhibited two pairs of redox waves [Fig. 2(c–e)]. During the CV scans, a green polymer film was formed on the working electrode surface. With increasing concentration of BFEE, the anodic oxidation potentials of BCHB were decreased in order. The nucleation process of the polymer was formed within a certain potential range. In other words, in the same potential range, the actual nucleation scope
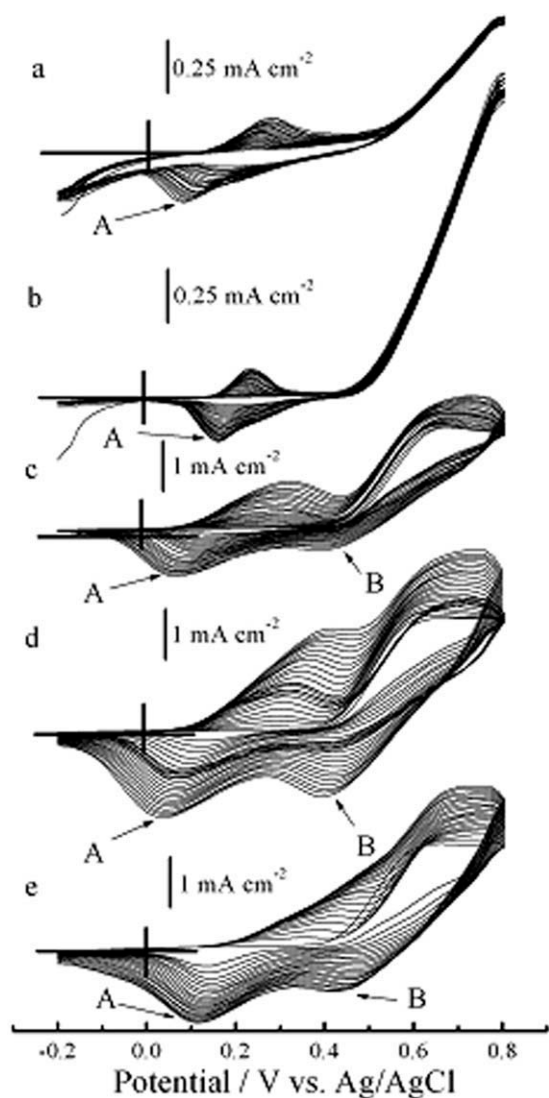
Figure 2 CVs of BCHB in CH_2Cl_2 with (a) 10, (b) 30, (c) 50, (d) 70, and (e) 90 vol % BFEE containing $0.05M$ monomers (potential scan rate = 100 mV/s).

was reduced with increasing anodic oxidation potentials. At the same potential range, from −0.2 to 0.8 V, as shown in Figure 2(a,b), the potential range was not enough to complete the nucleation process of the polycarbazole unit when the concentrations of BFEE decreased to 10 and 30%. It was displayed that the CVs of BCHB in CH_2Cl_2 with 10–30% BFEE exhibited only a single pair redox waves. For Figure 2(c–e), the average increase of peak A was a little bit higher than that of peak B; this indicated that more catechol units than carbazole units were incorporated onto the polymer main chain during the electrochemical polymerization. The reason was that the anodic oxidation potential onset of the catechol unit was lower than that of carbazole unit. The increase in the redox wave currents implied that the amount of the polymer on the electrode was increasing. It can also be seen in Figure 2(c–e) that the increase in

the redox wave current densities per cycle was the highest in CH_2Cl_2 with 70% BFEE [Fig. 2(d)]. On the basis of the results described previously, CH_2Cl_2 with 70% BFEE was chosen as the electrolyte for the electrosyntheses of PBCHB films.

Electrochemistry of the PBCHB films

To gain further insight into the electrochemical behaviors of the PBCHB films, the electrochemical properties of the PBCHB films deposited electrochemically from CH_2Cl_2 with 10, 30, 50, 70, and 90 vol % BFEE were also studied. The results are shown in Figure 3. The peak current densities were proportional to the scan rates (Fig. 3, insert); this indicated good redox behaviors of the polymers.[25–27] The CVs of PBCHB recorded in CH_2Cl_2 with 30, 50, 70, and 90 vol % [Fig. 3(b–e)] BFEE showed two pairs of redox peaks, O_1, R_1, and O_2, R_2. The first oxidation peak, O_1, resulted from the carbazole transition. The second peak, O_2, derived from the catechol transition. Furthermore, these polymer films were cycled repeatedly between the conducting (oxidized) and insulating (neutral) states without significant decomposition of the materials, indicating the high stability of the polymers. All these results indicate that the as-formed PBCHB films showed good redox activity and stability.

Structure characterization

The polymer synthesized electrochemically in CH_2Cl_2–70 vol % BFEE at a constant applied potential of 0.7 V was soluble in common organic solvents. The previous residual solution was washed with aqueous NaOH and then extracted between CH_2Cl_2 and deionized water. The combined extracts were dried with anhydrous $MgSO_4$ and evaporated. When the applied potential was increased to 1.0 V, the as-obtained PBCHB was insoluble in common organic solvents. The poor solubility of the polymers might have been due to their hyperbranched and crosslinked rigid network structures (Scheme 2).

Figure 4 displays the FTIR spectra of the BCHB monomer and the doped PBCHB prepared in CH_2Cl_2–70 vol % BFEE at 0.5, 0.7, and 1.0 V. The C—O stretching bands of BCHB and PBCHB prepared in CH_2Cl_2–70 vol % BFEE at different applied potentials were found at 1228, 1249, 1251, and 1253 cm^{-1}, respectively, as shown in Figure 4(a–d).[28] The absorption vibration band at 748 cm^{-1} indicated the existence of a 1,2-disubstituted benzene ring.[29,30] The band at 721 cm^{-1} was ascribed to the out-of-plane deformation vibration of the long alkyl chains [Fig. 4(a)].[20] After polymerization, the C—H vibration in alkyl still existed; this indicated that the hexyl chain was stable during the polymerization process. In
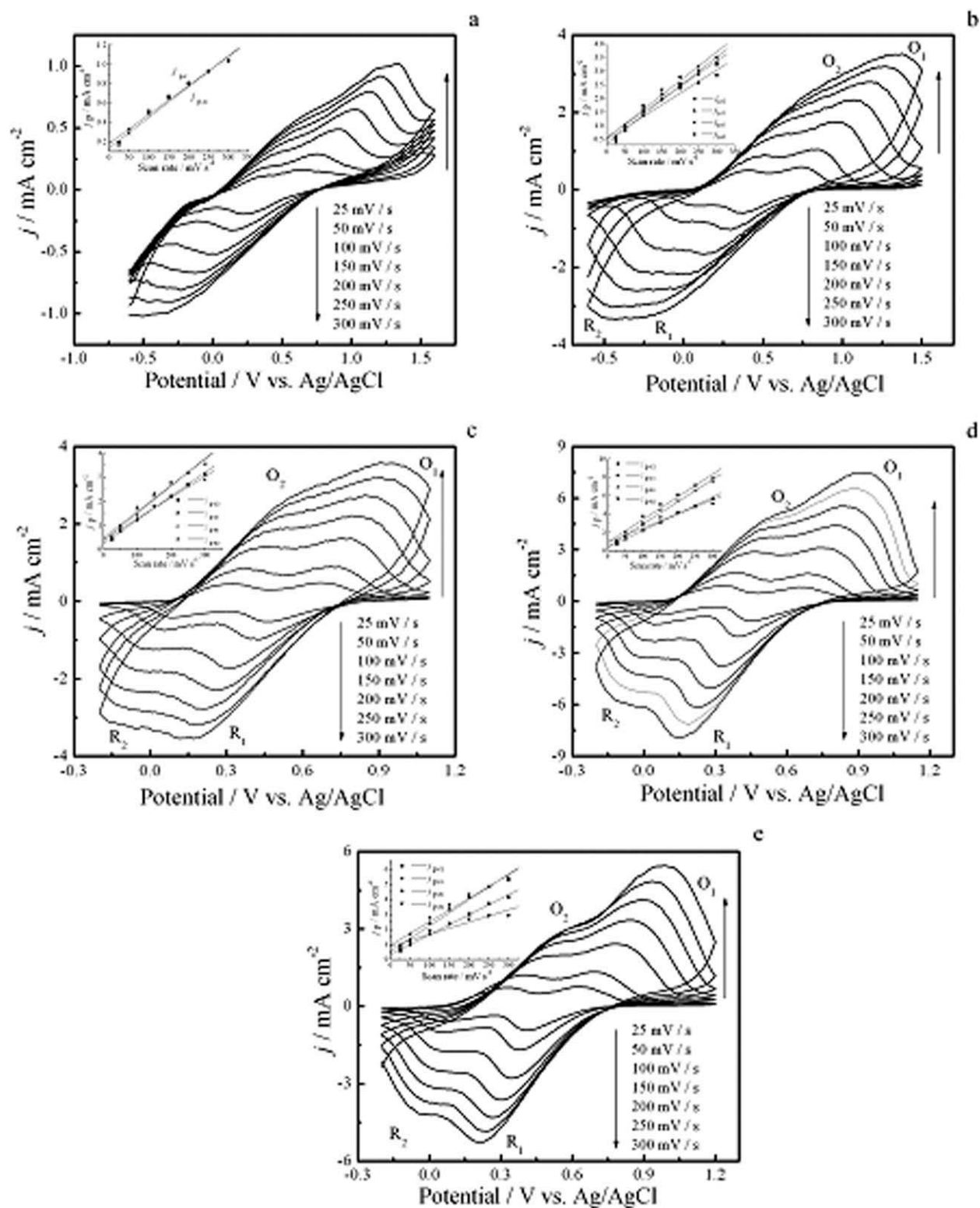
Figure 3 CVs of PBCHB film recorded in monomer-free CH_2Cl_2 with (a) 10, (b) 30, (c) 50, (d) 70, and (e) 90 vol % BFEE at different potential scan rates. The polymer films were electrodeposited in CH_2Cl_2 with 10, 30, 50, 70, and 90 vol % BFEE at a constantly applied potential of 0.9 V versus Ag/AgCl for 80 s, respectively.

contrast, the peaks at 748, 800, and 873 cm^{-1} [Fig. 4(b–d)] and 939 cm^{-1} [Fig. 4(d)] in the polymer spectra reflected the 1,2,4,5-substituted and 1,2,4-substituted benzene ring. These results imply that the elec-

tropolymerization of BCHB at constant applied potentials of 0.5 and 0.7 V occurred at the 1 position of the benzene ring on the catechol units (Scheme 2), whereas the polymerization at a constant applied
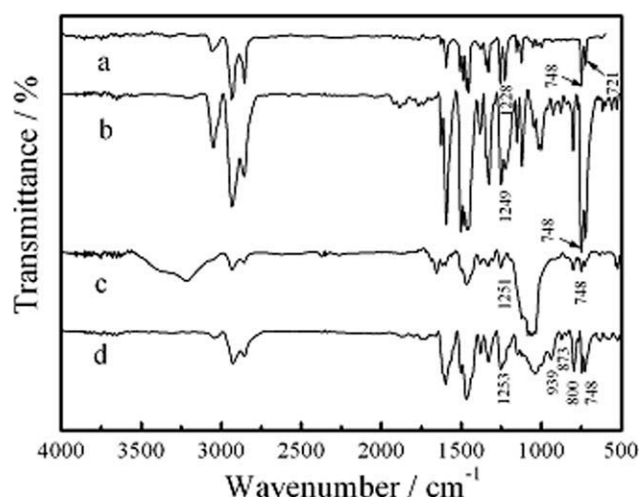
Figure 4 FTIR spectra of (a) BCHB and the doped PBCHB prepared in CH_2Cl_2–70 vol % BFEE at (b) 0.5, (c) 0.7, and (d) 1.0 V, respectively.

potential of 1.0 V occurred at the 1 position of the benzene ring on the catechol units and at the 11, 16 position or 12, 15 position of the benzene ring on the carbazole units (Scheme 2).

To further investigate the polymer structure and the polymerization mechanism of BCHB, the ^{1}H-NMR spectra of BCHB [Fig. 5(a)] and the doped polymer PBCHB [Fig. 5(b)] obtained from CH_2Cl_2–70 vol % BFEE at a constant applied potential of 0.7 V were recorded in $CDCl_3$. Generally, with the introduction of longer conjugation lengths into the polymer main backbone, the chemical shifts of hydrogen atoms on the aromatic rings move to lower fields. As can be seen in Figure 5, the proton lines of the polymer were broader than the corresponding proton lines of the monomer because of either the wide molar mass distribution or the complex structure of the polymer; this led to a slightly different environment of the atoms. The chemical shifts of C—H bonds in the ^{1}H-NMR spectra of BCHB are shown in Figure 5(a). In Figure 5(b), the chemical shift at δ = 8.11 arose from the protons at the C(13) and C(14) positions of the BCHB units. The three group peaks at δ = 7.36, 7.29, and 7.14 could be ascribed to the protons at the C(10) and C(17), C(11) and C(16), and C(12) and C(15) positions, which moved to δ = 8.11, 7.46, and 7.41, respectively, in the spectrum of the polymer. The chemical shift at δ = 6.81 was ascribed to the proton at the C(1) position of the BCHB monomer, which disappeared in the spectrum of PBCHB. However, the proton signals at δ = 6.78, 4.17, 3.87, 1.77, 1.68, 1.42, and 1.33 could be ascribed to C(2), C(9), C(4), C(5), C(8), C(6), and C(7) positions, respectively, which moved to δ = 8.01, 4.32, 4.12, 1.88, 1.64, 1.42, and 1.26, respectively, in the spectrum of the polymer. By integrating the peaks, we found that the polymerization of BCHB mainly

occurred at C(1); this was in good agreement with the FTIR spectra results.

The compositions of the PBCHB films were characterized by MALDI–TOF MS, as shown in Figure 6. As shown, MALDI–TOF MS revealed that the soluble polymer synthesized electrochemically at a constant applied potential of 0.7 V [Fig. 6(a)] was mainly composed of monomer (m/z = 606.011), dimer (m/z = 1210.175), and trimer (m/z = 1813.256) and the reprocessed residual solution [Fig. 6(b)] was composed of monomer (m/z = 609.067), dimer (m/z = 1212.203), and trimer (m/z = 1831.239). These results indicate that the soluble polymer and the reprocessed residual solution were both short-chain oligomers (1–3 repetitive units). Because of the higher anodic oxidation potential onset of the carbazole unit in comparison with that of the catechol unit, when the applied potential was 0.7 V, the electrochemical polymerization of BCHB only occurred on the catechol units. Moreover, two alkyl-9H-carbazole pendants of BCHB led to an increase in the intermolecular steric hindrance; therefore, only oligomers with no more than three repetitive units were obtained. Because of the special structure of the monomer BCHB, the PBCHB films obtained at the applied potential of 0.7 V were trimers at most, and the electropolymerization of the monomer only occurred on the catechol units. The intensity of the trimer peak shown in Figure 6(a) was much stronger than that shown in Figure 6(b); this indicated there were many more trimers in the films than in the reprocessed residual solution. The
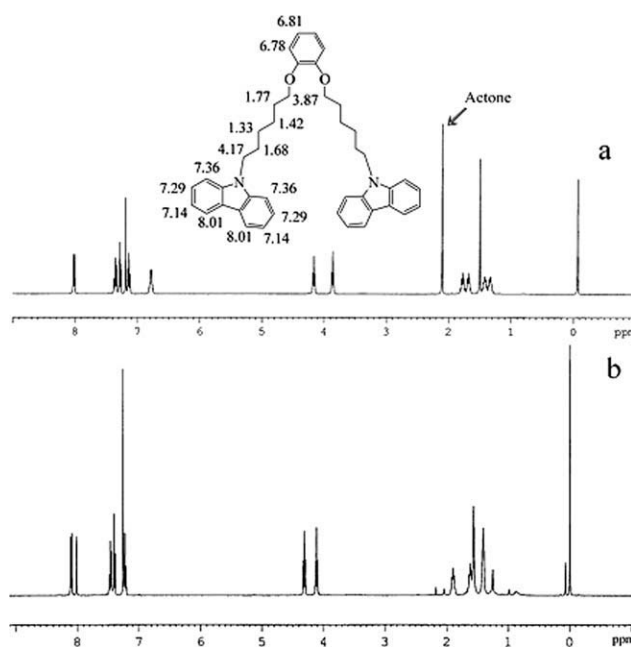

Figure 5 ^{1}H-NMR spectra of (a) BCHB and (b) the doped polymer PBCHB prepared in CH_2Cl_2–70 vol % BFEE at a constant applied potential of 0.7 V (solvent = $CDCl_3$).
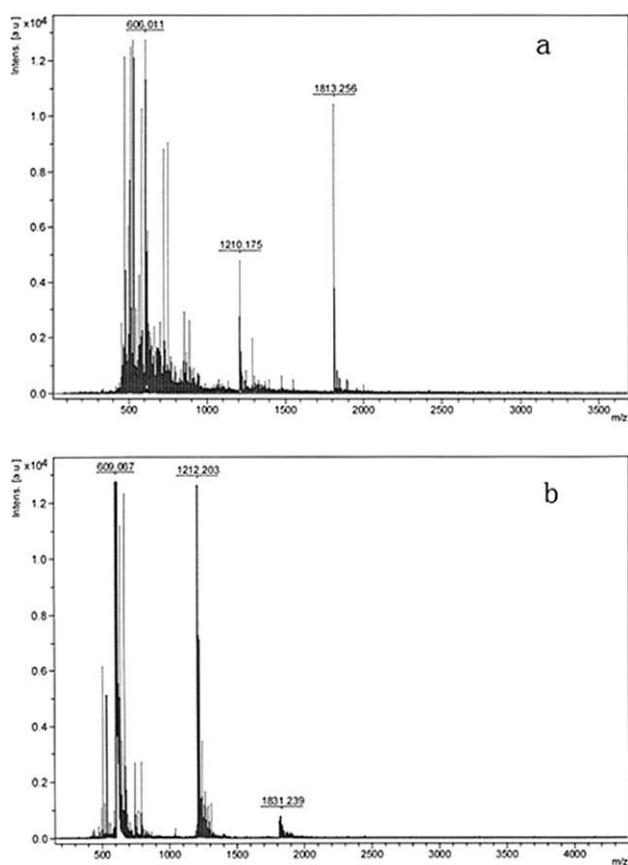
Figure 6 MALDI–TOF mass spectra of (a) the doped PBCHB film prepared in CH_2Cl_2–70 vol % BFEE at 0.7 V and (b) the reprocessed residual solution at 0.7 V (solvent = DMSO).

MALDI–TOF MS of soluble PBCHB at an applied potential of 1.0 V were also tested, although most PBCHB under these condition were insoluble in organic solvents. The results of the soluble PBCHB obtained at 1.0 V were almost in accordance with those at 0.7 V; this indicated similar structures of the polymers. We believe that the insoluble polymers synthesized electrochemically at 1.0 V were relatively high-molecular-weight polymers with high crosslinking degrees; this resulted in their insolubility. These phenomena demonstrated that the polymerization of the monomer at applied potentials smaller than 0.7 V happened preferentially on the catechol units, whereas when the applied potential was increased to 1.0 V, the polymerization could occur on both the catechol and carbazole units, and as a result, network structure films formed.

UV–vis and fluorescence spectra

The UV–vis spectra of the monomer BCHB in DMSO and the doped polymers PBCHB in the solid state on an ITO glass prepared in CH_2Cl_2–70 vol % BFEE at 0.5, 0.7, and 1.0 V were investigated, as
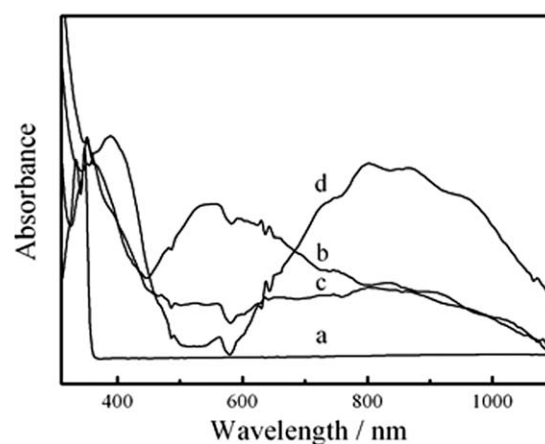

Figure 7 UV–vis spectra of (a) BCHB in DMSO and the doped PBCHB in the solid state prepared in CH_2Cl_2–70 vol % BFEE at (b) 0.5, (c) 0.7, and (d) 1.0 V.

shown in Figure 7. The monomer showed two characteristic absorption peaks at 333 and 348 nm [Fig. 7(a)]. On the other hand, in the doped state, the PBCHB films synthesized at 0.5, 0.7, and 1.0 V exhibited absorption peaks at 351 and 446–1100 nm [Fig. 7(b)], 350 and 485–1100 nm [Fig. 7(c)], and 388 and 503–1100 nm [Fig. 7(d)], respectively. Generally, the redshift of absorption indicates the formation of polymers with a higher conjugation length; this implied that PBCHB films prepared at 1.0 V had a relatively higher conjugation length compared with those prepared from the same system at 0.5 and 0.7 V and that of the monomer BCHB. The broad peaks could be assigned to the absorption of conductive species, such as polarons and bipolarons, on the main backbone of PBCHB in the doped state.
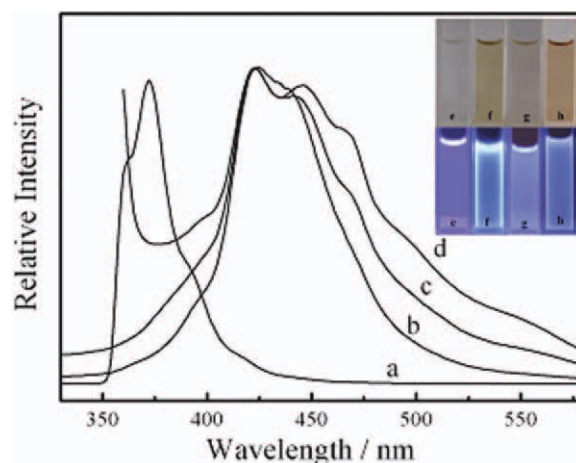

Figure 8 Fluorescence spectra of (a) BCHB in DMSO and the doped PBCHB in the solid state prepared in CH_2Cl_2–70 vol % BFEE at (b) 0.5, (c) 0.7, and (d) 1.0 V. Photoluminescence of (e) BCHB and the soluble PBCHB obtained at (f) 0.5, (g) 0.7, and (h) 1.0 V under UV light irradiation of 365 nm (insert; solvent = DMSO). [Color figure can be viewed in the online issue, which is available at wileyonlinelibrary.com.]
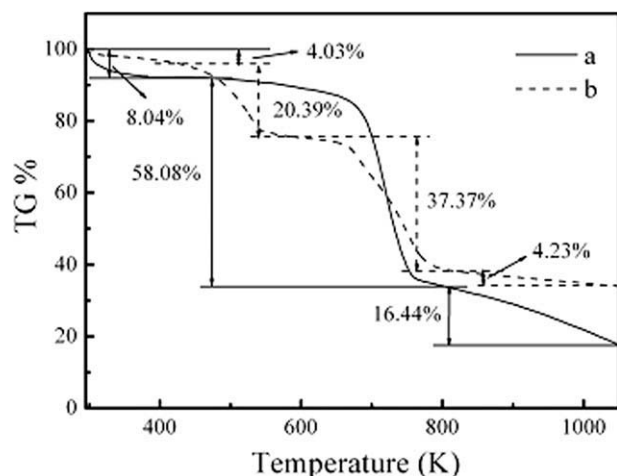
Figure 9 TGA curves of the doped PBCHB prepared in CH_2Cl_2–70 vol % BFEE at (a) 0.5 and (b) 1.0 V.

The fluorescence spectra of the monomer in DMSO and the doped polymer films in the solid state synthesized at 0.5, 0.7, and 1.0 and the photoluminescence of BCHB and the soluble PBCHB obtained at 0.5, 0.7, and 1.0 V under a UV-light irradiation of 365 nm are illustrated in Figure 8. The monomer exhibited a strong peak at about 372 nm, with a shoulder peak at 361 nm [Fig. 8(a)]. Compared to the monomer, the fluorescence spectra of the doped polymers had a 51-nm redshift with a maximum emission at 423 nm and a shoulder peak at 445 nm, which belonged to the emission of catechol units, whereas the doped polymers prepared at 0.7 and 1.0 V had a peak at 469 nm belonging to the

carbazole units. With the growth of the applied potentials, the peak at about 469 nm got stronger; this suggested that the content of polymers polymerized on both carbazole units significantly increased. From the fluorescence spectra of the polymers, we observed that the broad emission peaks overlaid the whole blue-light region. As shown in Figure 8, the soluble PBCHBs obtained at 0.5, 0.7, and 1.0 V in the doped states [Fig. 8(f–h)] exhibited a blue-light-emitting property, whereas the monomer showed much weaker emission [Fig. 8(e)]; this indicated that the polymer films prepared at different potentials were all blue-light emitters.

Thermal analysis

It is well known that the thermal properties of conducting polymers are quite important for their potential applications. To investigate the thermal properties of these polymers, TGA experiments were performed under a nitrogen stream in a temperature range of 295–1050 K with a heating rate of 10 K/min, as shown in Figure 9. As seen in the TG curves, there was a three-stage weight loss for PBCHB obtained at 0.5 V, and a four-stage weight loss for PBCHB was obtained at 1.0 V, respectively. For PBCHB prepared at 0.5 V [Fig. 9(a)], the first weight loss was slight from 295 to 473 K, up to 8.04%, and was due the evaporation of trace water or other moisture trapped in the polymer. The second one, up to 58.08%, from 473 to 805 K, could be ascribed to the degradation of the skeletal polycatechol

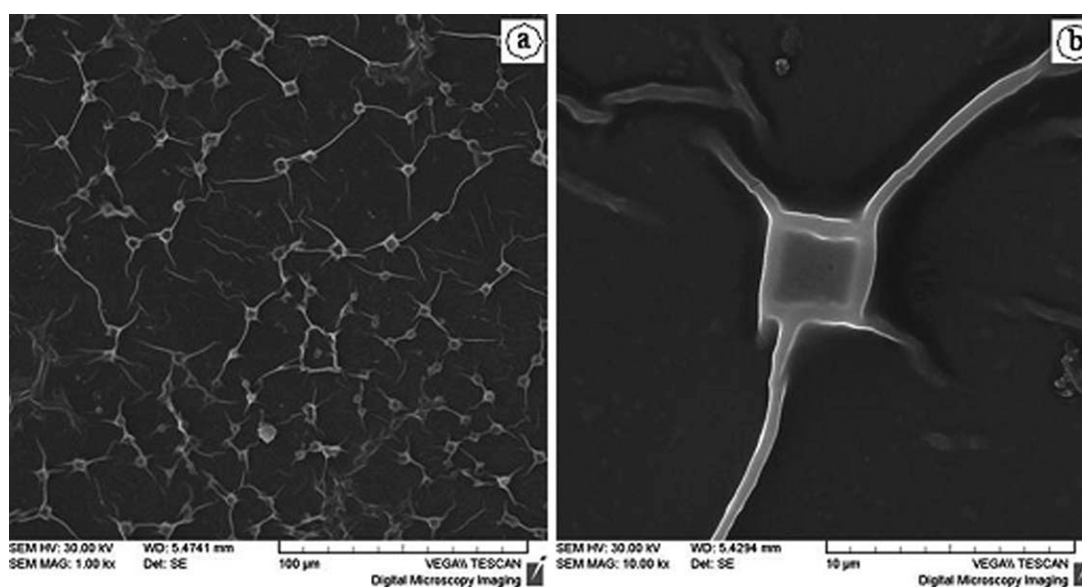**Figure 10** SEM micrographs of the dedoped PBCHB films at magnifications of (a) 1000 and (b) 10,000× on ITO electrode. The films were synthesized electrochemically in CH_2Cl_2–70 vol % BFEE at a constant applied potential of 1.0 V versus Ag/AgCl.

backbone structure. The last one, from 805 to 1050 K, up to 16.44%, probably resulted from the overflow of some oligomers decomposing from the polymers. On the other hand, for PBCHB prepared at 1.0 V [Fig. 9(b)], there was an improvement in its thermal properties compared with that obtained at 0.5 V. It exhibited a four-stage degradation with maximal weight losses of 4.03% at 427 K, 20.39% at 588 K, 37.37% at 819 K, and 4.23% at 1050 K. The first stage of degradation could have been due to the evaporation of trace water or other moisture trapped in the polymer. The second one was due to the pyrolysis of the skeletal polycarbazole backbone chain structure. The third one could have been due to the degradation of the skeletal polycatechol backbone, such as that in the second stage, of PBCHB obtained at 0.5 V. The last one might have been caused by the decomposition of some oligomers in the polymers. From these results, we could logically conclude that the PBCHB films prepared at different potential applications both had good thermal stability.

Morphology

The properties of conjugated polymers are strongly dependent on their morphology and structure. Therefore, Figure 10 presents the scanning electron micrographs of the PBCHB films prepared from CH_2Cl_2–70 vol % BFEE at a constant applied potential of 1.0 V. As shown in this figure, catenulate and lump structures were observed, which could be ascribed to the long alkyl chains increasing the steric hindrance between the carbazole groups of the monomer BCHB; then, the polymerization occurred between the molecules.

Nature of the linkages in the polymers

On the basis of the previously discussed results, two different electrochemical polymerization mechanisms of the monomer BCHB could be inferred (Scheme 2). The catechol and carbazole units in the monomer were labeled a and b, respectively. Because of the great distinction of the initial oxidation potentials between catechol and carbazole, it was very difficult to copolymerize catechol and carbazole with bands a and b. Most of the monomers were polymerized by bands of a–a modes at low potential (route A) to result in dimer and trimer. The monomers were crosslinked by bands of a–a, and b–b when the potential increased to 1.0 V (route B). The fraction of carbazole units formed the nature of crosslinkages due to carbazole monomer could easily polymerize into freestanding films. At the same time, some unpolymerized catechol and carbazole units remained at the end of the polymer chain.

CONCLUSIONS

The precursor monomer BCHB, which contained two pendent electroactive units, was designed and successfully synthesized, and PBCHB films were electrosynthesized by the direct anodic oxidation of BCHB at different potentials in CH_2Cl_2–70% BFEE with good redox activity and stability. UV–vis, FTIR spectroscopy, ^{1}H-NMR spectral analyses, and MALDI–TOF MS results determined that the electrochemical polymerization of BCHB at lower applied potentials (e.g., 0.5 and 0.7 V) preferentially occurred on the catechol units, and the polymers were soluble in common organic solvents. When the applied potential was increased to 1.0 V, the polymerization occurred both on catechol and carbazole units; this resulted in the formation of network polymer films, which were insoluble in any common organic solvents. The SEM results indicated that the PBCHB films had catenulate and lump structures. With these results, we concluded that the PBCHB films could be synthesized electrochemically on different polymerized units by control of the applied potentials. Furthermore, PBCHB showed stronger blue emissions at much longer wavelengths than their monomers because of the formation of conjugated polymers. With so many attractive properties, the PBCHB films showed great potential for organic light-emitting diodes and phosphorescent light-emitting diodes. The great versatility of materials will certainly be explored in future years for many optoelectronic applications. Light-harvesting devices and molecular electronics are the most likely fields of research that will take advantage of the great potential of polycarbazole-functionalized polycatechol materials.

References

1. Skotheim, T. A.; Reynolds, J.Conjugated Polymers: Processing and Applications; CRC: Boca Raton, FL, 2006.
2. Kickelbick, G.Hybrid Materials: Synthesis, Characterizations and Application; Wiley-Interscience: New York, 2007.
3. Nalwa, H. S. Handbook of Organic–Inorganic Hybrid Materials and Nanocomposites; American Scientific: California, 2003.
4. Bernier, P.; Lefrant, S.; Bidan, G.Advances in Synthetic Metals: Twenty Years of Progress in Science and Technology; Elsevier: Lausanne, Switzerland, 1999.
5. Leclerc, M.; Faid, K. Adv Mater 1997, 9, 1087.
6. Leclerc, M. J Polym Sci Part A: Polym Chem 2001, 39, 2867.
7. Maggie, A. Z. H.; Christopher, K. O. J Vac Sci Technol B 1998, 16, 3701.
8. Li, Y.; Vamvounis, G.; Holdcroft, S. Macromolecules 2002, 35, 6900.
9. Fukukawa, K.; Shibasaki, Y.; Ueda, M. Macromolecules 2004, 37, 8256.
10. Katz, H. E. Chem Mater 2004, 16, 4748.
11. Veres, J.; Ogier, S.; Lloyd, G.; Leeuw, D. D. Chem Mater 2004, 16, 4543.
12. Ma, M. L.; Liu, H. T.; Xu, J. K.; Li, Y. Z.; Wan, Y. Q. J Phys Chem C 2007, 111, 6889.

13. Laguna, A.; Ortíz, R.; Weinhold, E. Port Electrochim Acta 2007, 25, 285.
14. Chapuzet, J. M.; Simonet, J. Tetrahedron 1991, 47, 791.
15. He, J.; Crase, J. L.; Wadumethrige, S. H.; Thakur, K.; Dai, L.; Zou, S. Z.; Rathore, R.; Hartley, C. S. J Am Chem Soc 2010, 132, 13848.
16. Saraç, A. S.; Yavuz, Ö.; Sezer, E. Polymer 2000, 41, 839.
17. Saraswalchi, R.; Hillman, A. R.; Martin, S. J. J Electroanal Chem 1999, 460, 267.
18. Abe, S. Y.; Bernede, J. C.; Delvalle, M. A.; Tregouet, Y.; Ragot, F.; Diaz, F. R.; Lefrant, S. Synth Met 2002, 126, 1.
19. Taoudi, H.; Bernede, J. C.; Del Valle, M. A.; Bonnet, A.; Morsli, M. J Mater Sci 2001, 36, 631.
20. Wei, Z. H.; Wang, Q.; Xu, J. K.; Nie, Y. L.; Du, Y. K.; Xia, H. Y. J Polym Sci Part A: Polym Chem 2008, 46, 5232.
21. Nie, G. M.; Xu, J. K.; Zhang, S. S.; Han, X. J.; Pu, S. Z. J Appl Electrochem 2006, 36, 937.
22. Xu, H.; Xu, Z. F.; Yue, Z. Y.; Yan, P. F.; Wang, B.; Jia, L. W.; Li, G. M.; Sun, W. B.; Zhang, J. W. J Phys Chem C 2008, 112, 15517.
23. Chu, Z. Z.; Wang, D.; Zhang, C.; Fan, X.; Tang, Y. W.; Chen, L.; Zou, D. C. Macromol Rapid Commun 2009, 30, 1745.
24. Shi, G. Q.; Jin, S.; Xue, G.; Li, C. Science 1995, 267, 994.
25. Fritz, B.; Paul, R. Electrochim Acta 2000, 45, 2467.
26. Lu, G. W.; Shi, G. Q. J Electroanal Chem 2006, 586, 154.
27. Xu, J. K.; Zhang, Y. J.; Hou, J.; Wei, Z. H.; Pu, S. Z.; Zhao, J. Q.; Du, Y. K. Eur Polym J 2006, 42, 1154.
28. Lu, B. Y.; Zeng, L. Q.; Xu, J. K.; Le, Z. G.; Rao, H. Y. Eur Polym J 2009, 45, 2279.
29. Dong, B.; Zheng, L. Q.; Xu, J. K.; Liu, H. T.; Pu, S. Z. Polymer 2007, 48, 5548.
30. Xie, Y.; Jiang, F. X.; Xu, J. K.; Zeng, L. Q.; Dong, B.; Lu, B. Y.; Shang, X. X. Eur Polym J 2009, 45, 418.